ACS OMEGA

Open Access

http://pubs.acs.org/journal/acsodf

Article

Annealing Effect on Mechanical and Tribological Behaviors of Nanoscale Mechanics of $Zr_{60}Cu_{25}Al_5Ag_5Ni_5$ Thin-Layer Metallic Glasses for Engineering Materials Applications

Adem Ali Muhabie* and Wubshet Mekonnen Girma

Cite This: *ACS Omega* 2023, 8, 38204−38211

Read Online

ACCESS | Metrics & More | Article Recommendations | Supporting Information

ABSTRACT: A new and unique alloy formulation design strategy has been developed in order to fabricate thin-layered metallic glasses (TLMGs) with superior fracture resistance and low coefficient of friction (COF) during the nanoscratching test. Due to the outstanding properties, TFMG could be applied for different uses, such as for surface coating, biomedical, bioimprinting, electronic devices, spacecraft, and railway, all of which need surface fracture resistance. The fabricated Zr-based metallic glass was prepared from Zr, Al, Cu, Ni, and Ag above 99.9 Wt % in purity by arch melting techniques. TFMGs were coated on silicon wafer by sputtering the vapor deposition method from bulk metallic glass then annealed below glass transition temperature $T_g \sim 450$ °C for 10, 30, and 60 min. Nanoindentation and nanoscratch tests were used to investigate nanomechanical and nanotribological properties, and atomic force microscopy (AFM) was used to examine the surface morphology and microstructures of TLMG. The nanoindentation data indicated that the average hardness of metallic glasses increased from 9.75 (as-cast MG) to 13.4 GPa (annealed for 60 min). Coefficients of friction for the cast sample, annealed for unannealed, 10, 30, and 60 min, were 0.062, 0.049, 0.039, and 0.03, respectively, as well as the wear depths were 201.56, 148.43, 37.32, and 25.27 nm, respectively. These studies show that the coefficient of friction and wear rate decreases when the annealing time increases as a result of atomic reordering and structural relaxation that occurred at longer annealing times. Furthermore, continuous wear process, wear depth, wear track volume, and contact area decrease with increasing annealing time. This study can be used to design protocols to prepare novel TLMGs, which have outstanding mechanical and tribological properties for engineering materials applications.

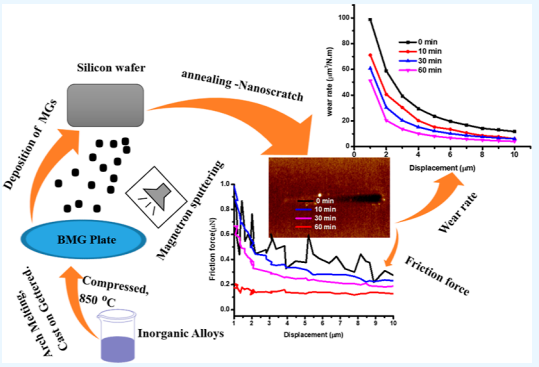

1. INTRODUCTION

Bulk metallic glasses (BMGs) are the focus of demanding research areas for researchers around the world.[1] BMGs are structurally amorphous metallic alloys, and their compositions are mixed to avoid crystallization during cooling from the melt.[2] BMGs exhibit extraordinary outstanding properties, such as high elasticity,[3] high hardness, appreciable toughness, good tribology prosperity,[4] and superior corrosion resistance.[5] In addition, due to the lack of long-range atomic order in BMGs, they exhibit exceptional mechanical and physicochemical properties,[6] related to conventional crystalline metallic materials, making them a promising class of engineering materials. Recent developments in surface-coating technology, particularly in the production of thin-film metallic glass on the substrate, there are various processing techniques,[7] such as physical vapor deposition (PVD), chemical vapor deposition (CVD), magnetron sputtering deposition, casting, and spin-coating, that have been investigated by researchers.[8] These techniques are used for the recent history of surface-coating technology developments in metallic glass−metal, ceramic−ceramic, ceramic−metal, and ceramic−metallic glass-nano-structured coatings. In thin-film material growth, recent advances in sputter-coating deposition and PVD have led to the improvement of superlattice and nanolayered films, which can normally have ultrahardness properties and surface fracture-resistance properties.[9] Plasma-assisted PVD is possibly an enormously advantageous method in the advancement of novel production of wear- and corrosion-resistant materials. Plasma-assisted PVD permits close regulators on the procedure parameters, with the resultant possibility to attain special nonequilibrium compositions and structures.[10] Recent researchers are interested in sputter PVD methods to generate nanocomposite coatings, which are superhard and corrosion/wear-resistant materials with accompanying great elastic moduli. Even though impressive efficiencies were shown

Received: June 22, 2023
Accepted: September 21, 2023
Published: October 5, 2023

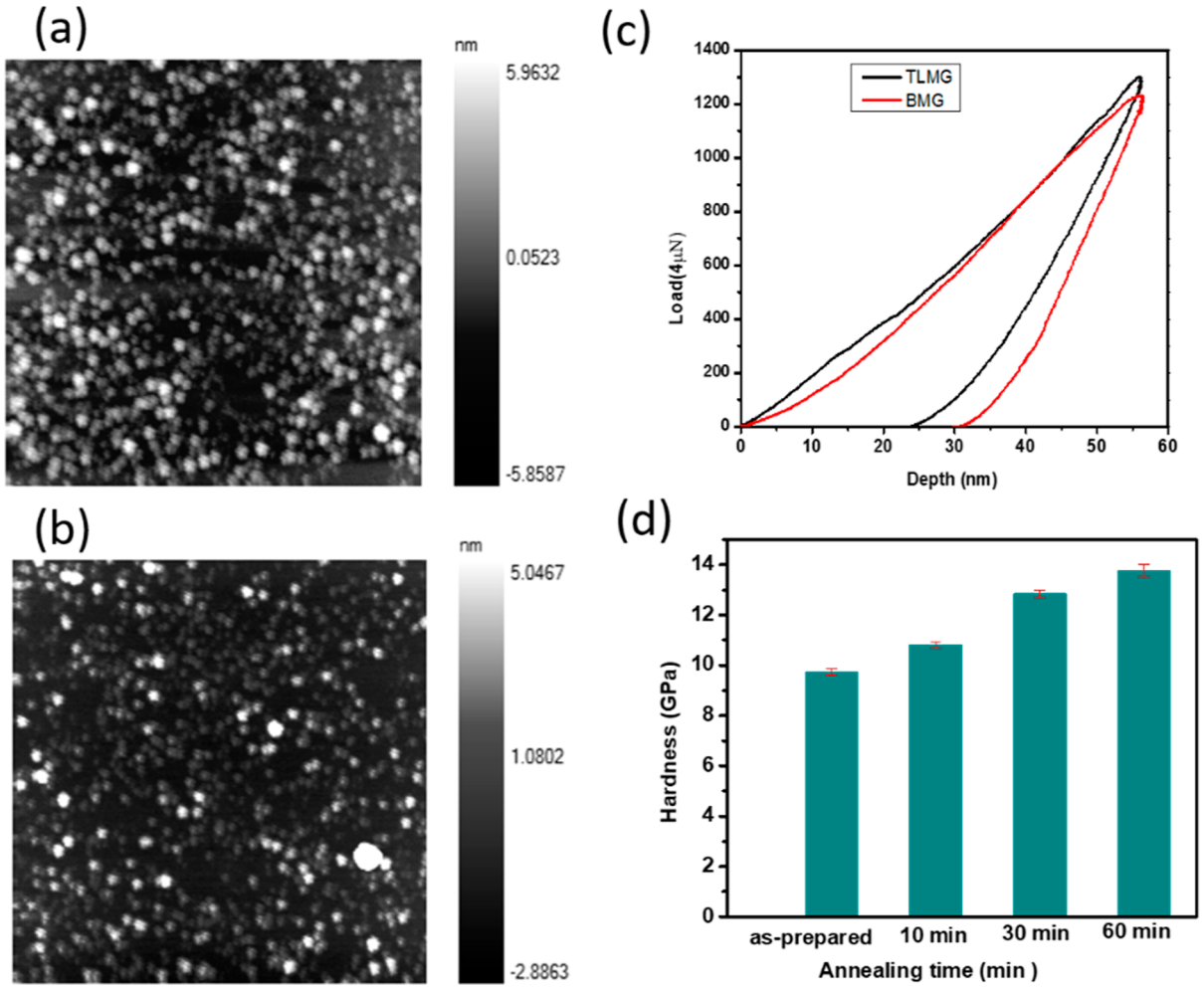

Figure 1. AFM image showing the microstructure of MG at annealing times of 30 (a) and 60 min (b). (c) Indentation profiles of TLMG and BMG. (d) Hardness of TLMGs for annealing times of 10, 30, and 60 min. Error bars represent the standard deviation of three replica experiments.

during laboratory tests for such materials, which may not be the ultimate solution for many commercial practical applications.[11] Moreover, even though the sputter PVD process is an outstanding method for the study of various coating surface nanostructures and compositions; other methods, for instance, electron-beam evaporative PVD could be commercially highly cost efficient, if evaporate source materials may be designed.[12] MGs are also novel wear-resistant[13] and low friction materials with a highly intensive demand in tribological applications.[14] Zr-based MGs display a smaller friction coefficient than other metals during dry sliding conditions.[15] In previously reported works, the wear resistance of CuZr-based MG materials is comparable to classical tribological ceramics but superior to that of high-performance steel.[16] Metallic glasses can be formed thermoplastically in the supercooled liquid regime. These special properties of MGs make them perfect candidates for multipurpose applications, such as microgears, media-storage devices,[17] building, construction, bioimplant,[18] and electrode materials,[19] energy conversion/storage,[20] and sensors.[21] Developing a proper alloy composition determines both structural and chemical homogeneities, nanometer-sized ductile dendrite homogeneities as a result of annealing have proven their value in increasing plasticity compared to the as-cast MG. The presence of such homogeneities promotes the plastic formability because they increase nucleation and branching.[22] At the macroscale, the tribological mechanisms are complex and involve a combination of plasticity,[23] transformation, and structural relaxations with structural changes.[24,25] There is no clear and unique correlation between the hardness/modulus and the tribological behavior of metallic glasses that has been established so far. Hence, the contributions of hardness, elastic modulus, and thermal treatment on wear resistance and nanoscale friction of thin MG compared to bulk and as-cast counterpart should be studied.[26] Furthermore, improper alloy composition of crystallites, rough surface, and surface reaction structural relations are the cause for their high friction, poor wear resistance, and poor plasticity, which limit the long-term performance of metallic glasses at ambient temperature.[27] In addition, localized and inhomogeneous decomposition at ambient temperature, free volume, and accompanied by strain lead to early failure of deformation, which still limits the long-term service of MGs for structural applications.[28] To avoid this catastrophic failure, this investigation aims to study mechanical properties like elastic moduli or hardness, inhomogeneity, and microstructure of metallic glasses in addition to thermal treatment which play great roles in providing information about the interrelation mechanism of nanoscale friction and nanoscale wear rate.

In this work, TFMG was grown on the surface of silicon substrate by the magnetron sputtering-coating deposition method from $Zr_{60}Cu_{25}Al_5Ag_5Ni_5$ BMG. Atomic force micros-

https://doi.org/10.1021/acsomega.3c04451
ACS Omega 2023, 8, 38204−38211

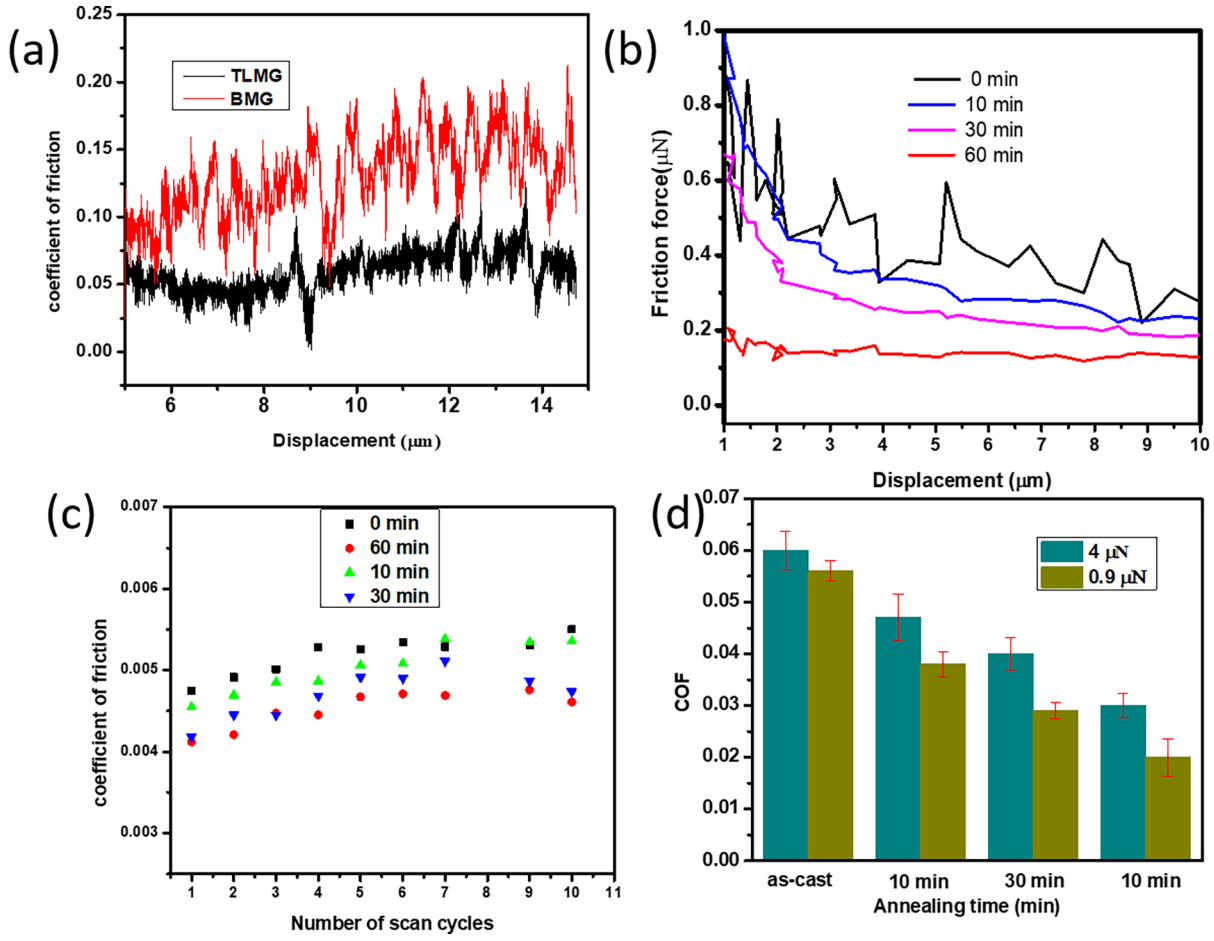

Figure 2. (a) Coefficient of friction for BMG and TLMG with displacement. (b) Friction force of TLMG at different annealing times. Coefficient of friction as a function of the number of scan cycles (c) and annealing time (d). Error bars represent the standard deviation of three replica experiments.

copy (AFM) was used to examine the surface morphology and microstructures. The nanotribological performance of the TFMGs were examined by the nanoscratch test, and the corresponding wear resistance and COF values were studied. We designed a proper alloy percent composition and characterized the structure and mechanical properties of thin-layer amorphous Zr-based MGs. The various annealing time effects and applied force changes on the morphological change, elastic modulus, hardness, wear rate, wear depth, and coefficient of friction of the samples were systematically investigated.

2. EXPERIMENTAL SECTION

2.1. Sample Preparation and Characterization Methods. $Zr_{60}Cu_{25}Al_5Ag_5Ni_5$ metallic glass was prepared by arch melting. The inorganic alloys of metals, such as Zr, Cu, Al, Ag, and Ni, above 99.9 Wt % in purity were mixed and cast on Zr-gettered. The cast alloys were placed on copper cruisers compressed with quartz at a temperature of 825 ± 25 °C. In order to ensure the composition homogeneity of metals in the metallic glass, melting of the alloy should be repeated five times. The final cast alloy has a plate shape structure with dimensions of 85 × 57 × 2.2 mm^3 (length, height, and width). 200 nm thick MGs were prepared on a silicon wafer by the magnetron sputtering deposition method from the plate. The as-cast samples were placed in vacuum quartz tubes and annealed for 10, 30, and 60 min under vacuum with Ti as an oxygen getter in a tubular iron-furnace below the glass transition, T_g ∼ 450 °C and at a maximum pressure of 3 × 10^{-5} mbar.[29,30] For comparison, one nonannealed sample representing as-prepared or as-cast samples was prepared. The samples were immediately removed from the furnace and cooled to room temperature. Structural relaxation happened due to thermal treatment below the glass-transition temperature of the alloy. The new design alloy composition of $Zr_{60}Cu_{25}Al_5Ag_5Ni_5$ with incorporation of Al, Ag, or Ni might be the best among glass-forming alloys.[31] Nanoindentation experiments were performed using a Hysitron Triboindenter TI-750 L (Hysitron, Inc., Minneapolis, MN USA) for 0.9 and 4 μN at a constant loading/unloading rate of 0.1 μN/s. Four indentations were performed to prove the accuracy of the data from the same sample. Nanoscratch tests were performed at a velocity of μm s^{-1} with applied forces of 0.9 and 4 μN as a function of displacement to evaluate the wear rate, wear depth, coefficient of friction, and contact area. During nanoscratch, the surface morphology and microstructures of the wear track were captured. Nanoscratch tests were repeated three times.

3. RESULTS AND DISCUSSION

3.1. Microstructures and Mechanical Properties. Annealing thin-layer metallic glass at various length times (10, 30, and 60 min) was selected as test parameters because of

https://doi.org/10.1021/acsomega.3c04451
ACS Omega 2023, 8, 38204−38211

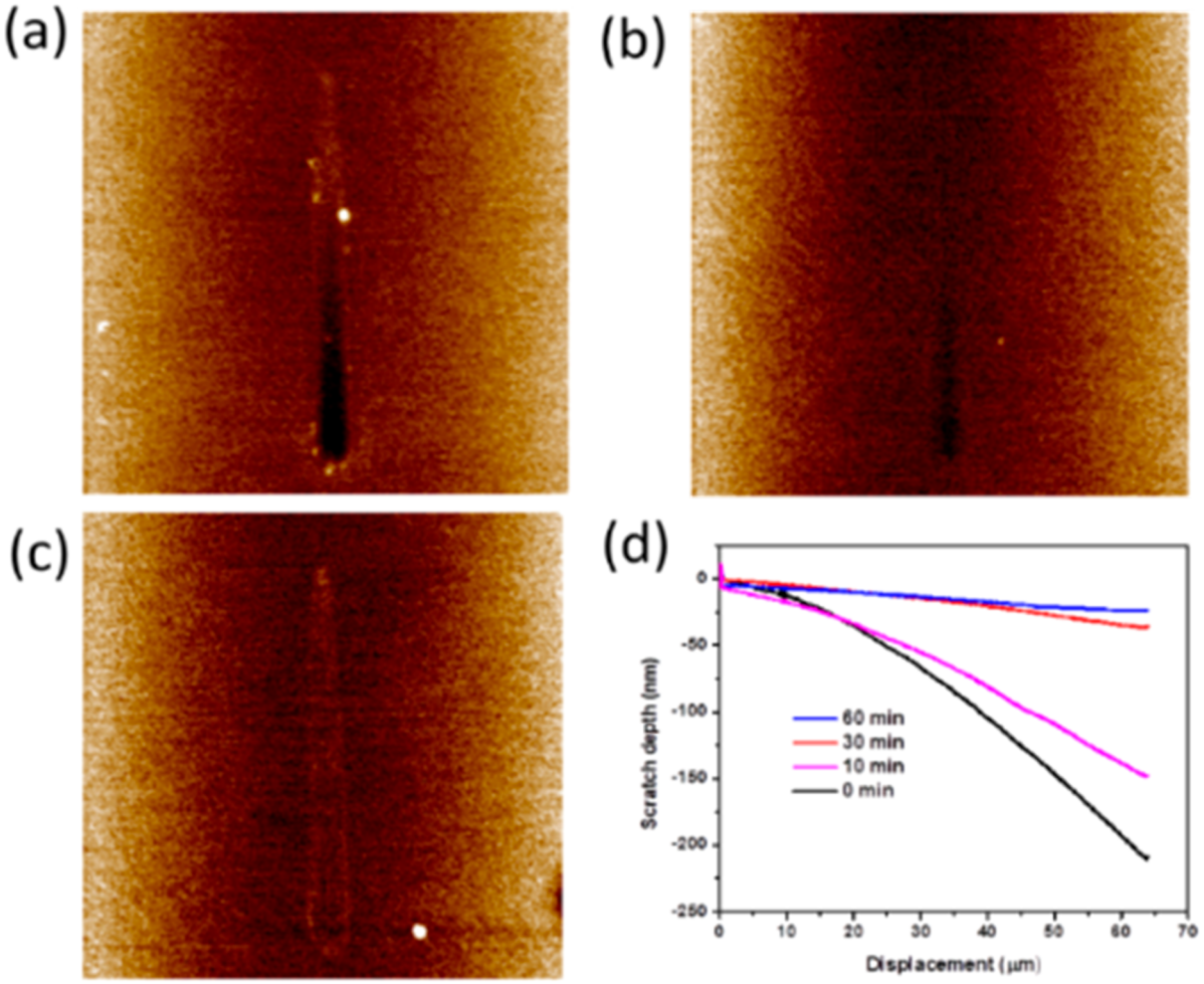

Figure 3. AFM images after nanoscratch tests over (a) as-cast TLMG and after annealing for (b) 30 and (c) 60 min at a normal force of 4 μN and the corresponding (d) wear depth of each sample at a load of 4 μN.

the differences in microstructure and mechanical and tribological properties of $Zr_{60}Cu_{25}Al_5Ag_5Ni_5$ TLMG. In order to explore the annealing effect on the microstructure and surface morphology, atomic force spectroscopy (AFM) has been used. The AFM images in Figure 1a,b clearly show the presence of nanoparticles with sizes of around 5.96 and 5.05 nm for the specimens annealed for 30 and 60, respectively. The images show the nanoscale inhomogeneity indicating chemical relaxation, with the evolution of atomic scale upon annealing below the glass transition temperature. The AFM topography results are in line with the previously reported results.[32] These local compositional fluctuations or random arrangements of atoms influence the plasticity of MGs, without a high loss of strength or hardness. The arrangement of atoms can affect atomic transport, hardness, elastic modulus, magnetic, wear rate, friction, and electrochemical properties.[13,33] Annealing results for chemical reordering leads to phase transition of MG, depending on the interatomic distance of atoms and improved plasticity of MG. Short interatomic distance between transition metals in the alloy composition may have existed only in the metallic glass.[34] Representative indentations on the BMG and TLMG of load−displacement curves are shown in Figure 1c. The surface indentation profiles show that the indented depth of TLMG is shallow compared with that of BMG, indicating lower material loss and higher wear resistance.

The depth dependence of the mechanical properties, the hardness (H), and elastic modulus (E) values of the MGs were determined for samples that were annealed for different times. The average hardness of metallic glasses increased from 9.75 to 13.4 GPa (Figure 1d) as the annealing time rose from zero to 60 min, as a result of atomic reordering and structural relaxation that occurred at longer annealing times. Atomic chemical ordering in the glassy phase is smaller than in the crystalline phase, which indicates the improvement of mechanical and tribological properties.[35] The elastic modulus improved from 142.49 to 162.64 with an increasing annealing time (figure S2). With respect to elastic behavior, describing the metallic glass properties not only by hardness and modulus but also by using a hardness/modulus (H/E) ratio indicating the elastic strain to failure.[2] The average H/E ratio was also increased as the annealing time increases, as shown Figure S3. The H/E ratio indicates the plasticity of sample deformation. Materials with a higher H/E ratio may reveal a structural transition from elastic to plastic behavior at higher stress levels compared to those with lower H/E ratios. H/E is a strong pointer of a good wear resistance of material. The large H/E value indicating that the material has high resist plastic deformation, and the most durable MGs can be used for many applications, which were annealed at different times individually to obtain heat-dependent surface properties. The

https://doi.org/10.1021/acsomega.3c04451
ACS Omega 2023, 8, 38204−38211

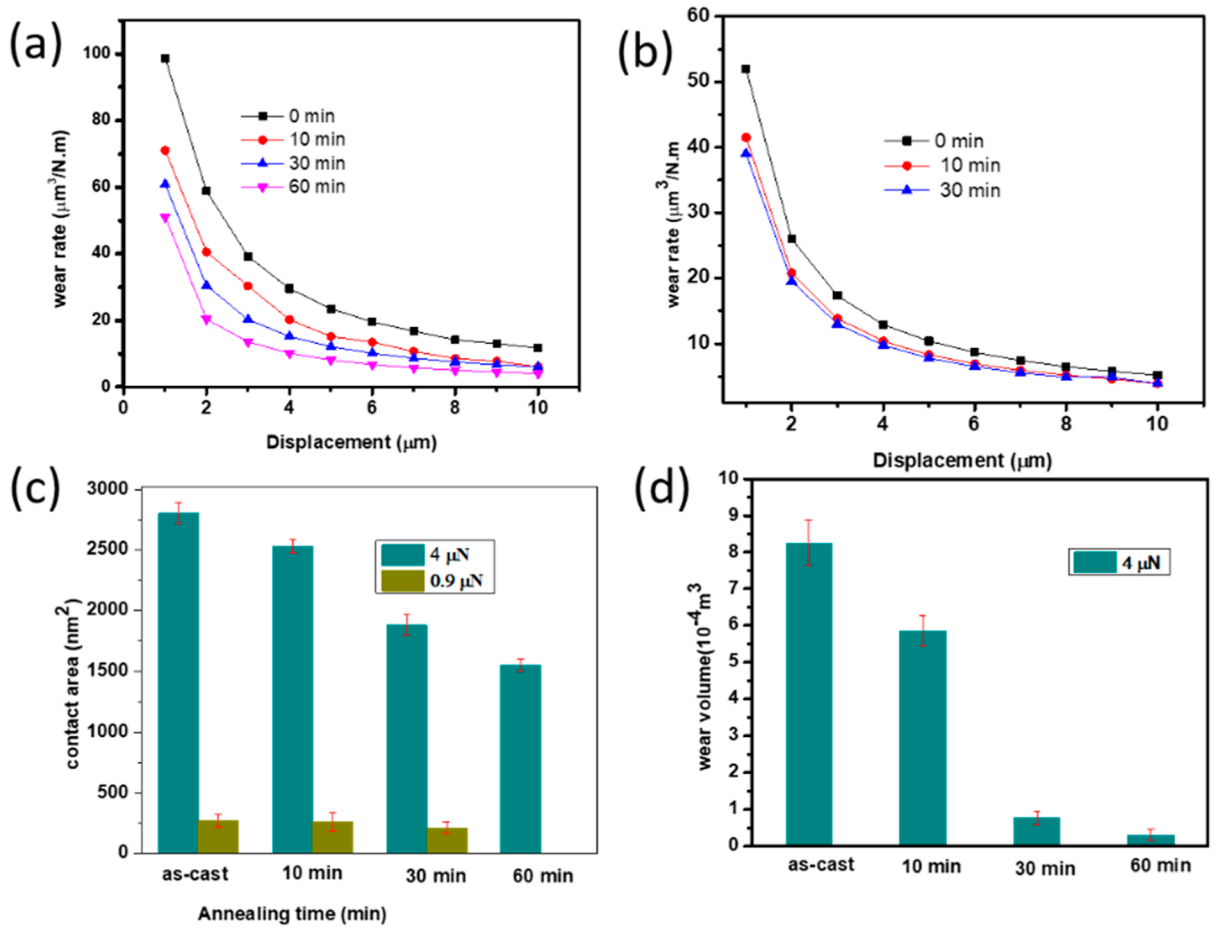

Figure 4. Wear rate as a function of annealing time for (a) 4 and (b) 0.9 μN. (c) Contact area as a function of annealing time for 0.9 and 4 μN. (d) Wear volume for each sample as a function of sliding displacement for 4 μN. Error bars represent the standard deviation of three replicate experiments.

mechanical properties observed in this research are comparable to the previous works.[2,36]

3.2. Tribological Properties. *3.2.1. Coefficient of Friction.* Figure 2 displays the behavior of friction of the thin-film metallic glass surface as a function of displacement, annealing time, and number of wear cycles. Friction coefficients of bulk and thin-layer metallic glass as a function of sliding displacement are shown in Figure 2a. The coefficient of friction is larger in bulk MG than in thin-film MGs. The sawtooth appearance of bulk MG is revealed, indicating shear banding and plow formation as the indenter deformed the matrix as a result of the absence of elastic plasticity. It might be difficult for the movement of atoms in all directions, while the indenter scratching the surface is due to the presence of some extent of crystallinity. As the annealing time increases, reducing the grain size, annealing-induced embrittlement of metallic glasses results in a lower friction coefficient and excellent wear resistance. Figure 2b demonstrates that for all annealed MGs, the reduction of friction force was observed as a function of sliding distance under load 4 μN. The value of friction force dropped gradually when the annealing time increased from zero to 60 min. The friction force of highly annealed MGs is much lower than that of the cast-MG. The graph of friction force for a cast MG revealed sawtooth, many small peaks, indicating the rough surface, deformation of surface matrix, and weak wear resistance performance, whereas the graph of highly annealed MG showed a smooth peak as increasing with annealing time indicating that the laminated surface and mechanical and tribology properties were successfully improved.[6,37] The coefficient of friction as a function of the number of scratch cycles after annealing for different times is shown in Figure 2c under an applied load of 0.9 μN. The coefficient of friction initially seems to increase with the number of wear cycles and then reaches a steady value at for all samples. The increase in the coefficient of friction during the initial wear cycle is related to a larger plowing depth, as reported previously.[38] In addition, the coefficient of friction of the thin-film MGs slightly decreases with increasing temperatures and aging times. The effects of annealing time on the coefficient of friction of thin-film MGs has been observed in Figure 2d under 0.9 and 4 μN applied force. The mean coefficient of friction value was similar for both test conditions. It is clear that the value of friction coefficient is about 0.062 for the nonannealed, while for the MG, it was annealed for 60 min, and the coefficient of friction slightly decreased (<0.03) under 0.9 μN applied force. The friction coefficient decreases with increasing annealing time in both conditions, which is in line with previous reports,[39] demonstrating the possibility of reduction of friction coefficient by tuning the surface patterning with aging temperature.[13] It is reported that most of the frictional work during the wear process creates heat energy, which modifies the tribological behaviors of Nano-scratched surfaces, such as forming delocalized free metal ions

https://doi.org/10.1021/acsomega.3c04451
ACS Omega 2023, 8, 38204−38211

for chemical reordering or even heating interfacial contact materials.[40]

3.2.2. Nanowear Depth. The nanoscratch test was conducted on the TLMGs, which were annealed at different times individually to obtain heat-dependent surface properties. Figure 3 shows the AFM images of the wear track surface of three MGs after the nanoscratch test using normal forces, 4 μN. All nanoscratch wear track images display different features in both FN = 0.9 and 4 μN loads. In addition, AFM images demonstrate different wear depth and contact area of MGs for different annealing times. Wide and deep grooves were shown (Figure 3a) for nonannealed MG but shallow scratch tracks were observed for highly annealed MGs (Figure 3c). The wear debris has been seen for as-cast, which are material accumulation on the lateral sides, indicating the serious plastic deformation during friction. The wear rate and volume weight loss for 4 μN were significantly higher than the 0.9 μN test conditions, which is in line with previous reports. The wear depth of each scratch sample is determined and shown in Figure 3d. The values of the wear depth decrease from 201.56 nm for the nonannealed to 148.43, 37.32, and 25.27 nm for the TLMG annealed for 10, 30, and 60 min, respectively, which is in line with previous reports. The nanoscratch wear track images of the three thin-film MGs at normal forces, 0.9 μN, are shown Figure S4. The wear depth is equivalent to both the height of the accumulated material and the depth of the scratch. It can be seen that the thin-layer MG, which is annealed for a long period of time, revealed a shallow wear track, indicating there is clearly elastic recovery behind the indenter and exhibited excellent wear resistance performance and very low coefficient of friction.[41] Wear resistance improved with annealing time increases, as a result of good hardness and elastic modulus of materials, which led to too much reduction of friction while plowing the MG layer on an indenter.[42] During annealing, antiwear and low coefficient of friction in all conditions improved on the surface of the film, and there might be dangling bonds (immobilized free radical); therefore, annealing needs to satisfy these bonds by surface reconstruction, charge transfer, or chemical absorption.[32,43,44]

3.2.3. Wear Rate. The variations of wear rate as a function of displacement for each samples at normal forces of 0.9 and 4 μN load are shown in Figure 4a,b, respectively. It is found that for all samples the wear rate first decreases and then steady-state wear is observed as a function of the sliding distance under both loads and all annealing time. The wear rate dropped continuously with increasing annealing time for both test conditions. The wear rates for 4 μN were meaningfully higher than 0.9 N test conditions, which is in line with previous works.[45] More importantly, the wear rate of the highly annealed MGs is much lower than that of the nonannealed MG. Figure 4c shows the contact area as a function of annealing time for 0.9 and 4 μN. As can be seen, the scratch contact area decreases with increasing annealing time for both loads. Contact areas for 4 μN were meaningfully higher than 0.9 N test conditions, which is in line with previous works. This behavior of the contact area depends on the mechanical properties (hardness and elastic modulus) and the microstructure of the film.[46]

Figure 4d shows the wear volume of the scratched area of samples for normal force, 4 μN. It is found that the wear volume decreases with increasing annealing time as a result of improved elastic modulus or high H/E ratio and low friction coefficient. This will be the reason for the high wear resistance of materials.[47] Researchers regarded that the real area of contact and material properties, such as microstructure, surface topography, and mechanical properties, are the key factors that govern the wear rate.[48] These findings might offer a promising protocol to enhance the wear resistance and lower the COF of the MG thin films by developing the proper alloy percent composition and appropriate annealing time below the perfect T_g value.

4. CONCLUSIONS

In summary, we have studied the surface morphology and microstructure by AFM, mechanical properties by the nanoindentation experiment, and tribological properties by the nanoscratch experiment of MG films annealed for various lengths of time. The hardness value and the average elastic modulus of the samples increased with increasing the annealing time, and the annealed samples revealed better properties than as-cast MG. The H/E ratio of all samples increased with increasing annealing time. The nanoscratch results indicate that annealing at different times significantly reduces friction and improves wear resistance performance. In addition, the decrease of wear depth, wear volume, and contact area under the annealing effect appeared in the continuous wear process, resulting in a lower coefficient of friction and good wear prevention performance, making MGs a promising material for applications in tribological materials, electrode materials, energy storage, and sensor applications.

■ ASSOCIATED CONTENT

Data Availability Statement

All data are included in this article. No other experimental data supporting this study.

Supporting Information

The Supporting Information is available free of charge at https://pubs.acs.org/doi/10.1021/acsomega.3c04451.

MGs (before and after annealing) obtained by AFM, MG annealed for 60 min , elastic modulus, E, values of the MGs annealed at 10, 30, and 60 min, average elastic modulus of metallic glass, H/E ratios of all samples , AFM images of the three thin-film MGs after the scratch test at normal forces, 0.9 μN, appearances of different features of the wear track, and shallow groove depths (PDF)

■ AUTHOR INFORMATION

Corresponding Author

Adem Ali Muhabie − *Department of Chemistry, Woldia University, Woldia 400, Ethiopia;* orcid.org/0000-0003-4609-5589; Email: alimohabe2003@gmail.com

Author

Wubshet Mekonnen Girma − *Department of Chemistry, Wollo University, Dessie 1145, Ethiopia;* orcid.org/0000-0003-3370-6731

Complete contact information is available at: https://pubs.acs.org/10.1021/acsomega.3c04451

Author Contributions

M.A. Ali designed the research, performed all experiments and wrote the manuscript. G.W. Mekonnen edited the paper. All authors discussed about the results and revised the manuscript on the paper.

https://doi.org/10.1021/acsomega.3c04451
ACS Omega 2023, 8, 38204−38211

Notes

The authors declare no competing financial interest.

■ ACKNOWLEDGMENTS

This work was financially supported by the Woldia University, Amhara Region, Ethiopia and by the National Taiwan University of Sciences and Technology, Department of Material Sciences and Engineering.

■ REFERENCES

(1) Zhao, X.; Sun, J.; Yu, M.; Zhang, M.; Liu, F.; Zhang, Y.; Liu, L. Effects of heat treatment on the thermal, mechanical and corrosion properties of deformed Zr-based bulk metallic glasses. *Mater. Chem. Phys.* **2020**, *256*, 123705.

(2) Li, M.-f.; Wang, D.-p.; Malomo, B.; Yang, L. Microstructural mechanisms of tuning the deformation behaviors in annealed metallic glasses. *J. Alloys Compd.* **2021**, *876*, 160029.

(3) Meylan, C.; Papparotto, F.; Nachum, S.; Orava, J.; Miglierini, M.; Basykh, V.; Ferenc, J.; Kulik, T.; Greer, A. Stimulation of shear-transformation zones in metallic glasses by cryogenic thermal cycling. *J. Non-Cryst. Solids* **2020**, *548*, 120299.

(4) Zhou, Q.; Du, Y.; Ren, Y.; Kuang, W.; Han, W.; Wang, H.; Huang, P.; Wang, F.; Wang, J. Investigation into nanoscratching mechanical performance of metallic glass multilayers with improved nano-tribological properties. *J. Alloys Compd.* **2019**, *776*, 447−459.

(5) Liang, D.; Tseng, J.-C.; Liu, X.; Cai, Y.; Xu, G.; Shen, J. Investigation of the structural heterogeneity and corrosion performance of the annealed Fe-based metallic glasses. *Materials* **2021**, *14* (4), 929.

(6) Salehan, R.; Shahverdi, H. R.; Miresmaeili, R. Effects of annealing on the tribological behavior of Zr60Cu10Al15Ni15 bulk metallic glass. *J. Non-Cryst. Solids* **2019**, *517*, 127−136.

(7) Jiang, L.; Bao, M.; Dong, Y.; Yuan, Y.; Zhou, X.; Meng, X. Processing, production and anticorrosion behavior of metallic glasses: A critical review. *J. Non-Cryst. Solids* **2023**, *612*, 122355.

(8) McGinn, P. J. Thin-film processing routes for combinatorial materials investigations—a review. *ACS Comb. Sci.* **2019**, *21* (7), 501−515.

(9) Comby-Dassonneville, S.; Venot, T.; Borroto, A.; Longin, E.; Der Loughian, C.; Ter Ovanessian, B.; Leroy, M.-A.; Pierson, J.-F.; Steyer, P. ZrCuAg thin-film metallic glasses: toward biostatic durable advanced surfaces. *ACS Appl. Mater. Interfaces* **2021**, *13* (14), 17062−17074.

(10) Yiu, P.; Diyatmika, W.; Bönninghoff, N.; Lu, Y.-C.; Lai, B.-Z.; Chu, J. P. Thin film metallic glasses: Properties, applications and future. *J. Appl. Phys.* **2020**, *127* (3), 030901.

(11) Kim, J. H.; Yoo, G. H.; Ryu, W. H.; Park, E. S.; Lee, G.-H. Fatigue-Induced Surface Modification of Zr-Based Metallic Glass under Environmental Conditions. *ACS Omega* **2022**, *7* (45), 41256−41265.

(12) Wang, C.; Chen, P.-J.; Hsueh, C.-H. Au-Based Thin-Film Metallic Glasses for Propagating Surface Plasmon Resonance-Based Sensor Applications. *ACS Omega* **2022**, *7* (22), 18780−18785.

(13) Jia, Q.; He, W.; Hua, D.; Zhou, Q.; Du, Y.; Ren, Y.; Lu, Z.; Wang, H.; Zhou, F.; Wang, J. Effects of structure relaxation and surface oxidation on nanoscopic wear behaviors of metallic glass. *Acta Mater.* **2022**, *232*, 117934.

(14) Ma, H.; Bennewitz, R. Nanoscale friction and growth of surface oxides on a metallic glass under electrochemical polarization. *Tribol. Int.* **2021**, *158*, 106925.

(15) Su, J.; Kang, J.-j.; Yue, W.; Ma, G.-z.; Fu, Z.-q.; Zhu, L.-n.; She, D.-s.; Wang, H.-d.; Wang, C.-b. Comparison of tribological behavior of Fe-based metallic glass coatings fabricated by cold spraying and high velocity air fuel spraying. *J. Non-Cryst. Solids* **2019**, *522*, 119582.

(16) Yao, J.; Wu, Y.; Sun, J.; Tian, J.; Zhou, P.; Bao, Z.; Xia, Z.; Gao, L. Friction and wear characteristics of silicon nitride ceramics under dry friction condition. *Mater. Res. Express* **2021**, *8* (3), 035701.

(17) Halim, Q.; Mohamed, N. A. N.; Rejab, M. R. M.; Naim, W. N. W. A.; Ma, Q. Metallic glass properties, processing method and development perspective: a review. *Int. J. Adv. Manuf. Technol.* **2021**, *112*, 1231−1258.

(18) Kiani, F.; Wen, C.; Li, Y. Prospects and strategies for magnesium alloys as biodegradable implants from crystalline to bulk metallic glasses and composites—A review. *Acta Biomater.* **2020**, *103*, 1−23.

(19) Lee, S.; Kim, S.-W.; Ghidelli, M.; An, H. S.; Jang, J.; Bassi, A. L.; Lee, S.-Y.; Park, J.-U. Integration of transparent supercapacitors and electrodes using nanostructured metallic glass films for wirelessly rechargeable, skin heat patches. *Nano Lett.* **2020**, *20* (7), 4872−4881.

(20) Amiri, A.; Shahbazian-Yassar, R. Recent progress of high-entropy materials for energy storage and conversion. *J. Mater. Chem. A* **2021**, *9* (2), 782−823.

(21) Chou Chau, Y.-F.; Chen, K.-H.; Chiang, H.-P.; Lim, C. M.; Huang, H. J.; Lai, C.-H.; Kumara, N. Fabrication and characterization of a metallic-dielectric nanorod array by nanosphere lithography for plasmonic sensing application. *Nanomaterials* **2019**, *9* (12), 1691.

(22) Wang, W. H. Dynamic relaxations and relaxation-property relationships in metallic glasses. *Prog. Mater. Sci.* **2019**, *106*, 100561.

(23) Ma, C.; Suslov, S.; Ye, C.; Dong, Y. Improving plasticity of metallic glass by electropulsing-assisted surface severe plastic deformation. *Mater. Des.* **2019**, *165*, 107581.

(24) Tao, K.; Li, F.; Liu, Y.; Pineda, E.; Song, K.; Qiao, J. Unraveling the microstructural heterogeneity and plasticity of Zr50Cu40Al10 bulk metallic glass by nanoindentation. *Int. J. Plast.* **2022**, *154*, 103305.

(25) Hasannaeimi, V.; Muskeri, S.; Gwalani, B.; Hofmann, D. C.; Mukherjee, S. Deformation behavior of metallic glass composites and plasticity accommodation at microstructural length-scales. *Mater. Today Commun.* **2020**, *24*, 101237.

(26) He, T.; Lu, T.; Ciftci, N.; Tan, H.; Uhlenwinkel, V.; Nielsch, K.; Scudino, S. Mechanical properties and tribological behavior of aluminum matrix composites reinforced with Fe-based metallic glass particles: Influence of particle size. *Powder Technol.* **2020**, *361*, 512−519.

(27) Hua, N.; Zhang, X.; Liao, Z.; Hong, X.; Guo, Q.; Huang, Y.; Ye, X.; Chen, W.; Zhang, T.; Jin, X.; et al. Dry wear behavior and mechanism of a Fe-based bulk metallic glass: description by Hertzian contact calculation and finite-element method simulation. *J. Non-Cryst. Solids* **2020**, *543*, 120065.

(28) Jiang, X.; Song, J.; Fan, H.; Su, Y.; Zhang, Y.; Hu, L. Sliding friction and wear mechanisms of Cu36Zr48Ag8Al8 bulk metallic glass under different sliding conditions: dry sliding, deionized water, and NaOH corrosive solutions. *Tribol. Int.* **2020**, *146*, 106211.

(29) Li, N.; Xu, E.; Liu, Z.; Wang, X.; Liu, L. Tuning apparent friction coefficient by controlled patterning bulk metallic glasses surfaces. *Sci. Rep.* **2016**, *6* (1), 39388.

(30) Li, J.; Gittleson, F. S.; Liu, Y.; Liu, J.; Loye, A. M.; McMillon-Brown, L.; Kyriakides, T. R.; Schroers, J.; Taylor, A. D. Exploring a wider range of Mg-Ca-Zn metallic glass as biocompatible alloys using combinatorial sputtering. *Chem. Commun.* **2017**, *53* (59), 8288−8291.

(31) Khan, M. M.; Nemati, A.; Rahman, Z. U.; Shah, U. H.; Asgar, H.; Haider, W. Recent advancements in bulk metallic glasses and their applications: a review. *Crit. Rev. Solid State Mater. Sci.* **2018**, *43* (3), 233−268.

(32) Zhou, Q.; Han, W.; Luo, D.; Du, Y.; Xie, J.; Wang, X.-Z.; Zou, Q.; Zhao, X.; Wang, H.; Beake, B. D. Mechanical and tribological properties of Zr-Cu-Ni-Al bulk metallic glasses with dual-phase structure. *Wear* **2021**, *474*−*475*, 203880.

(33) Alvi, S.; Milczarek, M.; Jarzabek, D. M.; Hedman, D.; Kohan, M. G.; Levintant-Zayonts, N.; Vomiero, A.; Akhtar, F. Enhanced Mechanical, Thermal and Electrical Properties of High-Entropy HfMoNbTaTiVWZr Thin Film Metallic Glass and its Nitrides. *Adv. Eng. Mater.* **2022**, *24* (9), 2101626.

(34) Louzguine-Luzgin, D. V.; Jiang, J. Low-temperature relaxation behavior of a bulk metallic glass leading to improvement of both strength and plasticity. *Mater. Sci. Eng., A* **2022**, *839*, 142841.

https://doi.org/10.1021/acsomega.3c04451
ACS Omega 2023, 8, 38204−38211

(35) He, R.-r.; Li, M.-f.; Malomo, B.; Yang, L. Enhancing corrosion and mechanical properties of 304 stainless steel by depositing and annealing Zr75Cu25 thin-film metallic glass. *Surf. Coat. Technol.* **2020**, *400*, 126221.
(36) Bignoli, F.; Rashid, S.; Rossi, E.; Jaddi, S.; Djemia, P.; Terraneo, G.; Li Bassi, A.; Idrissi, H.; Pardoen, T.; Sebastiani, M.; et al. Effect of annealing on mechanical properties and thermal stability of ZrCu/O nanocomposite amorphous films synthetized by pulsed laser deposition. *Mater. Des.* **2022**, *221*, 110972.
(37) Bajpai, S.; Nisar, A.; Sharma, R. K.; Schwarz, U. D.; Balani, K.; Datye, A. Effect of fictive temperature on tribological properties of Zr44Ti11Cu10Ni10Be25 bulk metallic glasses. *Wear* **2021**, *486*−*487*, 204075.
(38) Ye, W.; Du, P.; Xiao, S.; Li, M. Effect of annealing temperature on properties of WS2 thin films. *Surf. Eng.* **2022**, *38* (4), 411−416.
(39) Yi, X.; Feng, X.; Huang, B.; Sun, K.; Meng, X.; Gao, Z.; Zhang, Y.; Wang, H. The effect of annealing temperatures on the phase constitutes, thermal properties and corrosion behaviors of Ti-Ni-Zr-Cu high entropy alloy thin ribbons. *J. Alloys Compd.* **2022**, *896*, 162947.
(40) Ma, X.; Ma, J.; Bian, X.; Tong, X.; Han, D.; Jia, Y.; Wu, S.; Zhang, N.; Geng, C.; Li, P.; et al. The role of nano-scale elastic heterogeneity in mechanical and tribological behaviors of a Cu-Zr based metallic glass thin film. *Intermetallics* **2021**, *133*, 107159.
(41) Zhou, Q.; Luo, D.; Hua, D.; Ye, W.; Li, S.; Zou, Q.; Chen, Z.; Wang, H. Design and characterization of metallic glass/graphene multilayer with excellent nanowear properties. *Friction* **2022**, *10* (11), 1913−1926.
(42) Deng, L.; Gebert, A.; Zhang, L.; Chen, H.; Gu, D.; Kühn, U.; Zimmermann, M.; Kosiba, K.; Pauly, S. Mechanical performance and corrosion behaviour of Zr-based bulk metallic glass produced by selective laser melting. *Mater. Des.* **2020**, *189*, 108532.
(43) Kang, S.; Rittgen, K. T.; Kwan, S.; Park, H.; Bennewitz, R.; Caron, A. Importance of surface oxide for the tribology of a Zr-based metallic glass. *Friction* **2017**, *5* (1), 115−122.
(44) Liu, X.; Wang, T.; Wang, Q.; Song, X.; Liang, Y.; Feng, S.; Yang, F.; Chen, X.; Kong, J. Shear band evolution related with thermal annealing revealing ductile-brittle transition of Zr35Ti30Be27. 5Cu7. 5 metallic glass under complex stress state. *Intermetallics* **2022**, *140*, 107378.
(45) Ge, Y.; Cheng, J.; Zhang, B.; Xue, L.; Hong, S.; Wu, Y.; Liang, X.; Zhang, Z.; Zhang, X. Sliding wear behaviors of the AlNiTi amorphous coatings: effect of temperatures. *J. Mater. Res. Technol.* **2022**, *21*, 2362−2374.
(46) Wang, T.; Zhou, Y.; Zhang, L. Chemical and structural heterogeneity improve the plasticity of a Zr-based bulk metallic glass at low-temperature annealing. *J. Non-Cryst. Solids* **2023**, *603*, 122115.
(47) Wang, Q.; Zhou, Y.; Wu, P.; Qu, C.; Wang, H. Effect of laser surface structuring on surface wettability and tribological performance of bulk metallic glass. *Crystals* **2022**, *12* (5), 748.
(48) Marimuthu, K. P.; Han, G.; Lee, H. Multilayer thin film metallic glasses under nanoscratch: Deformation and failure characteristics. *J. Non-Cryst. Solids* **2023**, *601*, 122047.

https://doi.org/10.1021/acsomega.3c04451
ACS Omega 2023, 8, 38204−38211